

Journal Pre-proof

Development of NIR-HSI and chemometrics process analytical technology for drying of beef jerky

Eva M. Achata, Carlos Esquerre, K. Shikha Ojha, Brijesh K. Tiwari, Colm P. O'Donnell



PII: S1466-8564(21)00012-6

DOI: <https://doi.org/10.1016/j.ifset.2021.102611>

Reference: INNFOO 102611

To appear in: *Innovative Food Science and Emerging Technologies*

Received date: 14 December 2018

Revised date: 28 April 2020

Accepted date: 5 January 2021

Please cite this article as: E.M. Achata, C. Esquerre, K.S. Ojha, et al., Development of NIR-HSI and chemometrics process analytical technology for drying of beef jerky, *Innovative Food Science and Emerging Technologies* (2021), <https://doi.org/10.1016/j.ifset.2021.102611>

This is a PDF file of an article that has undergone enhancements after acceptance, such as the addition of a cover page and metadata, and formatting for readability, but it is not yet the definitive version of record. This version will undergo additional copyediting, typesetting and review before it is published in its final form, but we are providing this version to give early visibility of the article. Please note that, during the production process, errors may be discovered which could affect the content, and all legal disclaimers that apply to the journal pertain.

© 2021 Published by Elsevier.

Development of NIR-HSI and chemometrics process analytical technology for drying of beef jerky

Eva M. Achata¹, Carlos Esquerre¹, K. Shikha Ojha², Brijesh K. Tiwari^{2*}, Colm P. O'Donnell¹

¹School of Biosystems and Food Engineering, University College Dublin, Belfield, Dublin 4, Ireland

²Department of Food Chemistry & Technology, Teagasc Food Research Centre, Ashtown, Dublin 15, Ireland

Abstract

Beef jerky samples immersed in brine or water, both with and without ultrasound treatment were dried at 60 °C for 30, 60, 90, 120, 150, 180, 210 and 240 min. Drying behaviour was evaluated using ten drying kinetic models and hyperspectral imaging. All samples reached water activity values (A_w) < 0.85 during the first 90 min of drying. Moisture content (MC) of beef jerky was predicted using near infrared hyperspectral imaging and chemometrics. Partial least squares regression, band selection and spectral pre-treatments were applied to develop MC prediction models using beef jerky spectra. Most of the MC prediction models developed in this work had RPD values > 4, indicating their suitability for process control applications. The best performing MC prediction models for the non-ultrasound and ultrasound treated samples were developed using the ensemble Monte Carlo variable selection (EMCVS) on second derivative of $\log(1/R)$ spectra and EMCVS-selectivity ratio on linear detrended $\log(1/R)$ spectra, respectively. This study demonstrated the potential of NIR-HSI and chemometrics as a PAT tool for drying of beef jerky.

Key words: PAT, Near Infrared Hyperspectral imaging, Chemometrics, Jerky, Drying, Ultrasound, Beef, Brining.

1. Introduction

The process analytical technology (PAT) framework is defined as a mechanism to design, analyse and control manufacturing processes through the measurement of critical process parameters (CPPs) which affect critical quality attributes (CQAs) of raw and in-process materials and processes (Cullen, O'Donnell, & Fagan, 2014; Food and Drug Administration, 2004). PAT tools provide real-time information, facilitating manufacture of products with consistent quality and reduced waste, while lowering processing costs. PAT is widely employed in the pharmaceutical and chemical industries (Cullen, et al., 2014). However, there is a need to validate PAT tools for food industry applications to facilitate increased adoption of PAT in food manufacture.

Drying is a common and longstanding method of food preservation. Prediction of drying kinetics under different conditions may be employed to optimize the drying process which influences the quality of the dried food (Andueza, Agabriel, Constant, Lucas, & Martin, 2013; Luckose, Pandey, & Harila, 2017). Modelling of the drying process is important for equipment design, process optimization and product quality improvement (Zhao, Downey, & O'Donnell, 2014).

Jerky is a dried salted meat product with low water activity and a high protein to moisture ratio. Salt addition contributes to the preservation, characteristic taste and texture of jerky products. Various thin layer kinetic models have been investigated for drying of meat and meat products (Luckose, et al., 2017). Moisture content is the main factor influencing quality, safety and shelf life of the meat-based jerky products. Traditional methods for moisture content determination are time consuming, and not suitable for online monitoring of the drying process. Therefore, the development of a non-destructive rapid technology to monitor the drying process would facilitate the adoption of a process analytical technology

approach in jerky manufacture. (Achata, Esquerre, O'Donnell, & Gowen, 2015; Andersen, Frydenvang, Henckel, & Rinnan, 2016).

Ultrasound (US) technology has the potential to enhance drying processes by reducing the drying time and energy consumption (Corrêa, Rasia, Mulet, & Cárcel, 2017; Nian, Zhao, O'Donnell, Downey, Kerry, & Allen, 2017; Zhao, Downey, & O'Donnell, 2015). US has been reported to improve drying of fruits and vegetables (Corrêa, et al., 2017; Kowalski & Rybicki, 2017; Kroehnke, Szadzińska, Stasiak, Radziejewska-Kubzdela, Biegańska-Marecik, & Musielak, 2018; Magalhães, et al., 2017; Rojas & Augusto 2018; Tao, et al., 2018).

However limited studies have been reported on the drying of meat products in combination with US treatment (K. S. Ojha, Granato, Rajuria, Barba, Kerry, & Tiwari, 2018; S. K. Ojha, Kerry, & Tiwari, 2017). US can intensify mass transport phenomena in solid – liquid systems (Spellman, McEvoy, O'Cuinn, & FitzGerald, 2003). Application of US has been studied for brining of pork meat at different NaCl concentrations (Kuehler & Stine, 1974), and to improve the diffusion of NaCl in pork meat using different brining treatments (Siró, Vén, Balla, Jónás, Zeke, & Friedrich, 2009).

Near infrared hyperspectral imaging (NIR-HSI) is a rapid non-destructive technology that does not require sample preparation, and is a suitable process analytical technology tool for on/at-line control and monitoring of food processes (Huang, Yu, Xu, & Ying, 2008; Karunathilaka, Yakes, He, Chung, & Mossoba, 2018; Lieske & Konrad, 1996). NIR spectroscopy is well suited to moisture content determination because of strong water absorption bands in the NIR spectrum. Hyperspectral imaging (HSI) provides both spatial and spectral information of samples by combining imaging and spectroscopic tools. Chemometric methods are employed for the extraction of chemical information from hyperspectral images or hypercubes and to develop prediction maps for quality attributes.

Hyperspectral imaging has been investigated for the control of drying of banana slices (Slattery & Fitzgerald, 1998), mango slices (Kumar & Barth, 2010) and potato slices (Cadet, Pin, Rouch, Robert, & Baret, 1995). However the use of HSI to monitor the drying process of beef jerky has not been reported.

Chemometric tools used for hyperspectral imaging data analysis include principal component analysis (PCA), which is frequently employed as an exploratory tool and for dimensionality reduction (Burger & Gowen, 2011). Calibration techniques such as partial least squares regression (PLS-R) are routinely employed in hyperspectral imaging analysis for prediction of unknown concentrations and generation of prediction maps to estimate spatial distribution of components in a sample (A. Gowen, Burger, Esquerre, Downey, & O'Donnell, 2014). Band selection methods have been demonstrated to improve the performance of hyperspectral imaging models and to reduce the processing times required by selecting the most informative spectral bands (Achata, Inguglia, Esquerre, Tiwari, & O'Donnell, 2019) and have been studied for the early detection of bruise damage in mushrooms (C. Esquerre, Gowen, Downey, & O'Donnell, 2011), viability and vigour in muskmelon seeds (Karmali, Karmali, Teixeira, & Curto, 2004) fat and moisture content in ground beef (Schindler, Le Thanh, Lendl, & Kellner, 1998), internal damage in cucumbers and whole pickles (Resa & Buckin, 2011), evaluation of mixing quality of food powders (Achata, Esquerre, Gowen, & O'Donnell, 2018) and the assessment of the brining process for pork meat (Achata, et al., 2019). Spectral pre-treatments can be used to correct for the effects of natural variability in the shape and size of samples, light scattering and differences in the effective path length in NIR spectra, which can cause difficulties in the application of HSI for quality assessment (C. Esquerre, Gowen, Burger, Downey, & O'Donnell, 2012). Prediction models with RPD values > 3.5 are considered very good for process control applications of materials which have complex physical characteristics (Williams, 2014) such as meat samples.

The aim of this study was to investigate the development of NIR-HSI and chemometrics as a process analytical technology for drying of beef jerky.

2. Materials and methods

2.1. Sample preparation

Six fresh eye of round beef cuts (*M. Semitendinosus*) were purchased from local supermarkets. Beef cuts' batch codes were checked to ensure that each eye of round came from a different batch code. Fat and external connective tissue was removed from each eye of round cut and stored at -18 °C. Prior to analysis samples were maintained at 4 °C for 16 hours, sliced into 3 mm thick slices and trimmed to obtain uniform samples of ca. 75 mm × 65 mm × 3 mm. Two eye of round cuts were used per replicate.

2.2. Sample treatments

Four experimental treatments (water immersed (WI), brined (B), ultrasound treated and water immersed (US-WI), ultrasound treated and brined (US-B)) were carried out for 1 h at room temperature in 10 % NaCl (w/w) brine or distilled water. After immersion samples were blot dried. Control samples were not immersed in either water or brine. 5 groups of 26 slices were obtained (n = 130) from two eye of round cuts. Each group was assigned as control, WI, B, US-WI or US-B samples. From each group of 26 slices, 24 slices were used for drying studies and 2 slices were used for moisture content determination. The 24 slices for drying studies were divided into 8 groups of 3 slices. Samples from each group were weighed and hyperspectral images acquired before and after drying for selected periods. Three replicates of each treatment were carried out giving a total of 360 samples (5 (4 treatments and control)

x 24 (8 drying times x 3 samples/drying time) x 3 replicates). Ultrasonic treatments at an ultrasonic power of 100 W and frequency of 25 kHz were carried out using an ultrasonic bath (Ultrasonic TI-H-5; Elma Schmidbauer GmbH, Germany) maintained at 25°C using a temperature-controlled water jacket. A plastic container with 900 g of water or brine and 26 samples (24 for drying and 2 for moisture content determination) was positioned at the centre of the ultrasonic bath for 1 h treatment times.

2.3. Drying of beef jerky

Control and treated samples were dried at 60 °C for 30, 60, 90, 120, 150, 180, 210 and 240 min in a hot air-drying oven (3926TW, Excalibur, Sacramento, Ca. USA). At each drying time, a group of 3 samples was removed from the oven and cooled to room temperature prior to hyperspectral imaging and water loss determination.

2.4. Moisture content determination

Initial moisture content of control and treated samples was determined in duplicate using the standard AOAC reference method 950.46. (Altas, Kudryashov, & Buckin, 2016).

2.5. Modelling of drying kinetics

Ten thin layer kinetic models were evaluated to find the most suitable one to describe the drying kinetics of the beef jerky samples (Appendix 1). The moisture ratio (MR) was calculated as $(M-M_e)/(M_o-M_e)$, where M is the moisture content of the sample, M_e is the equilibrium moisture content (considered as 0) and M_o is the initial moisture content. Moisture content was expressed on a dry basis (kg of water/kg of dry matter). The best fitting

model was selected by comparing the correlation coefficient (R^2), reduced chi-square (χ^2 , Eq. (1)), root mean square error (RMSE (Eq. 2)) and the Akaike information criterion (AICc, Eq. (3)) of the fitted models.

$$\chi^2 = \left[\sum_{i=1}^N (MR_{exp,i} - MR_{pre,i})^2 \right] \div [N - n] \quad (1)$$

$$RMSE = \sqrt{\frac{1}{N} \sum_{i=1}^N (MR_{pre,i} - MR_{exp,i})^2} \quad (2)$$

$$AICc = 2n - 2 \log_e (\mathcal{L}(\theta^*|y)) + 2n(n+1)N - n - 1 \quad (3)$$

where, N is the number of observations, n is the number of constants in the model, $MR_{pre,i}$ is the i th predicted moisture ratio value and $MR_{exp,i}$ is the i th experimental moisture ratio value (Jones, Upson, Haugland, Panchuk-Voloshina, Zhou, & Haugland, 1997; Vega-Gálvez, Puente-Díaz, Lemus-Mondaca, Miranda, & Torres, 2014).

2.6. Near infrared hyperspectral imaging (NIR-HSI)

Hyperspectral images of fresh and dried samples were acquired at room temperature using a line scanning NIR-HSI system (DV Optics, Padova, Italy) in reflectance mode (spectral range of 880 – 1720 nm, spectral resolution of 7 nm and spatial resolution 0.3×0.3 mm pixel size). Image acquisition and calibration procedure was performed as reported by Achata, Esquerre, O'Donnell, & Gowen, 2015. HSI data were saved in ENVI formatted files and imported into Matlab (The MathWorks Inc., Natick, MA, USA) for further chemometric analysis.

2.7. Hyperspectral imaging data analysis

Hyperspectral data pre-processing and analysis was performed using in-house developed functions and scripts. The following spectral pre-processing was performed prior to calculation of sample mean spectra:

- Spectra were trimmed to a spectral range of 957 - 1664 nm to remove noise effects at both ends of the spectra.
- Dead pixels and spikes were replaced by the mean values of adjacent bands in the same spectrum.
- The background was removed using a mask, which was created by the difference between bands 1300 and 1510 nm > 0.1 .
- Hypercubes were unfolded by rearranging the three-dimensional hypercubes (X, Y, λ) into a two-dimensional matrix (X * Y, λ) to facilitate algorithm development.
- The mean reflectance spectrum from each jerky slice was obtained by averaging the spectral signals of all remaining pixels.
- Mean reflectance spectra was smoothed using the Savitzky-Golay (SG) 5 points second order polynomial method. Smoothed mean reflectance spectra were used for subsequent chemometric analysis.

PCA was carried out to investigate the relationships between experimental treatments and spectral data, and to identify potential outliers using the Hotelling T^2 statistic. A sample was considered as an outlier if the T^2 value was $> T^2_{crit} = A \times F_{(0.05, A, n - A)} \times (n-1)/(n-A)$, where A is the number of significant components, n is the number of spectra in the dataset and $F_{(0.05, A, n - A)}$ is the F statistic (with $\alpha = 0.05$, A and $n - A$ degrees of freedom). Regression models for moisture content prediction of non-ultrasound (non-US) (control, WI and B) and ultrasound (US-WI and US-B) treated samples were developed separately based on PCA exploratory analysis (not shown). Spectral data from 2 replicates were assigned to calibration sets to construct the regression models (144 non-US (48 control + 48 WI + 48 B) and 96 US (48 US-WI + 48 US-B) treated samples). Data from the third replicate was used to build the validation sets to test the models (72 non-US (24 control + 24 WI + 24 B) and 48 US (24 US-WI + 24 US-B) treated samples).

PLS-R models were evaluated using the full spectral range with and without pre-treatments, and selected bands. A range of spectral pre-treatments and combinations of any two of them (FD, first derivative; LD, linear detrend; SD, second derivative; TD, third derivative; SNV, Standard normal variate; AsLS, asymmetric least squares; MS, median scaled) were evaluated. The regression models were developed using both reflectance (R) and pseudo absorbance ($\log(1/R)$) spectra.

Band selection methods based on PLS were evaluated in pre-treated spectra. Variable importance in projection (VIP) (Chong & Jun, 2005; Munera, Amigo, Blasco, Cubero, Talens, & Aleixos, 2017), selectivity ratio (SR) (Rajalahti, Arneberg, Kroksveen, Berle, Myhr, & Kvalheim, 2009), ensemble Monte Carlo variable selection (EMCVS) (Achata, et al., 2018; C. A. Esquerre, Gowen, O'Gorman, Downey, & O'Donnell, 2017) were evaluated and compared with the use of VIP and SR values instead of regression coefficient vector in an ensemble of Monte Carlo procedure (EMCVS-VIP, EMCVS-SR respectively) to select the most informative bands.

The number of latent variables (LV), were selected by analysis of the root mean square error of ten-fold cross-validation ($RMSE_{CV}$) and roughness of the regression vector (A. A. Gowen, Downey, Esquerre, & O'Donnell, 2011). The performance of the regression models was assessed using the root mean square error (RMSE), the coefficient of determination (R^2) and the ratio of standard error of prediction to standard deviation (RPD) for calibration, full cross-validation, and prediction sets.

PLS method is described by Eq. (4) where \hat{y} is the estimated value using the model, X is the mean centred matrix of predictors, where each row corresponds to a sample and each column to a predictor, and β is the regression coefficient vector calculated for the number of latent variables.

$$\hat{y} = X\beta \quad (4)$$

The VIP method is one of the most widely used variable selection methods based on PLS. The VIP method assesses the contribution of each variable according to the variance explained by each PLS component (Hammami, et al., 2010).

The selectivity ratio compares the explained variance ($SS_{i,explained\ SR}$) with the residual variance ($SS_{i,residual\ SR}$) of each predictor variable, after the orthogonal variance to the response has been removed by combining the PLS components into a target-projected single axis (direction of the maximum variability of response variable) (Rajalahti, et al., 2009).

Then the selectivity ratio is calculated as:

$$t_{tp} = \frac{Xb}{\|b\|} \quad (5)$$

$$p_{pt} = \frac{X't_{tp}}{t_{tp}'t_{tp}} \quad (6)$$

$$SR_i = \frac{SS_{i,explained\ SR}/(n-2)}{SS_{i,residual\ explained\ SR}/(n-2)} = \frac{\|t_{tp}p_{tp,i}'\|^2(n-3)}{\|x_i - p_{tp,i}t_{tp,i}\|^2(n-2)} \quad (7)$$

The EMCVS calculates the mean of the standardised regression coefficients (\bar{C}_j) for each variable in an ensemble of K (K = 200 in this study) Monte Carlo procedures. For each Monte Carlo procedure β were calculated N times using M randomly selected samples to calculate the normalised regression coefficient (C_{jk}) as in Eq. (8).

$$C_{jk} = \frac{\bar{\beta}_{jk}}{s(\beta_{jk})} \quad (8)$$

$$\bar{\beta}_{jk} = \left(\sum_{i=1}^N \frac{\beta_{ijk}}{N} \right) \quad (9)$$

$$S(\beta_{jk}) = \left(\sum_{i=1}^N \frac{\beta_{ijk} - \bar{\beta}_{jk}}{N-1} \right) \quad (10)$$

Where $\bar{\beta}_{jk}$ and $S(\beta_{jk})$ are the mean and standard deviation of the regression coefficient of the j th variable ($j = 1, 2, 3, \dots, p$) over N times ($N = 200$ for this study) of all PLS runs and β_{ijk} is the regression coefficient for the j th variable in the i th PLS model ($i = 1 \dots N$) for the k th Monte Carlo procedure ($k = 1 \dots K$). EMCVS was applied iteratively until no more variables were removed from the data set (C. A. Esquerre, et al., 2017).

The β was replaced by VIP and SR vectors in Eq. (8) to Eq. (10) for EMCVS-VIP and EMCVS-SR methods.

A set of 100 evenly distributed thresholds between 0 and the maximum absolute VIP, SR or \bar{C} value was tested. Variables with value $>$ the threshold were retained. In each case the PLS model with the best performance was identified.

3. Results and discussion

3.1. Drying of beef jerky

3.1.1. Moisture content and drying kinetics

The mean moisture content of the three replicates used for the kinetic models is listed in Appendix 1. The moisture content (kg water/kg dry matter) during drying for all experimental treatments is presented in Fig. 1a. A gradual reduction in moisture content is observed during the first 90 min of drying, when free or loosely bound water is evaporated. Thereafter the drying curves level off as more strongly bound water is removed. All samples exhibited similar drying profiles. US-WI samples had the highest drying rate during the first 30 min of drying. Fig. 1b shows the predicted moisture ratio (MR) profiles during drying time for all experimental treatments. The goodness of fit of the 10 drying kinetic models evaluated are

presented in Appendix 2. The Newton model was the best fitting model for control, WI and US-B samples, while the logarithmic and the Page model were the best fitting models for the B and US-WI samples respectively. The MR of all samples decreased exponentially during the first 90 min of drying indicating that the diffusion rate of beef jerky slices was high at the start of the drying process for all samples. The remaining water after 90 min drying was strongly bound to the jerky tissue matrix. The observed results are in accordance with results reported in previous studies on the drying kinetics of cultured and uncultured beef jerky (S. K. Ojha, et al., 2017) and on the drying of beef and chicken meat using ultrasound treatment (Başlar, Kılıçlı, Toker, Sağdıç, & Arıcı, 2014).

3.2. Spectral characteristics of the beef jerky

Fig. 2 presents mean $\log(1/R)$ smoothed spectra of samples at selected drying times for each experimental treatment. For all experimental treatments, characteristic water peaks at 978 and 1454 nm may be observed. These prominent bands are due to a combination of symmetric and antisymmetric O–H stretching and bending modes (Lin & Brown, 1992). The peak at 978 nm becomes less prominent during drying and almost unnoticeable after 90 minutes of drying for the control and non-US (WI and B) treated samples. For the US-WI samples, a similar behaviour is observable after 60 min of drying indicating that ultrasound treatment enhances drying. Previous studies indicated that ultrasound pre-treatment can enhance drying rate in cherry tomatoes (Fernandes, Rodrigues, García-Pérez, & Cárcel, 2016), carrots and lemon peel (García-Pérez, Cárcel, Benedito, & Mulet, 2007). A large and broad absorbance peak at 1454 nm (Fig. 2) reduced during drying revealing an absorbance peak at around 1510 – 1517 nm which may be related to the N-H stretching first overtone linked to protein (Senesi, et al., 2009). The 1510 – 1517 nm protein peak may be observed earlier in control, WI and US-WI samples during drying (drying time \leq 120 min) compared to B and US-B samples indicating

that brining reduces the drying rate by increasing the water holding capacity of the jerky slices (Alarcon-Rojo, Carrillo-Lopez, Reyes-Villagrana, Huerta-Jiménez, & Garcia-Galicia, 2018). Absorbance peaks at 1888 - 1195 nm may be related to the C-H stretching second overtone (Osborne, Fearn, & Hindle, 1993).

3.3. Regression models

Five samples identified as outliers using the T^2 statistic were removed from the data sets before model development. EMCVS, SR, VIP, EMCVS-SR and EMCVS-VIP were evaluated to develop MC prediction models for beef jerky samples (Control, WI, B, US-WI, US-B.). The best performing models were selected from 50 developed models for each regression method evaluated (section 2.6.2), using both reflectance (R) and logarithmic transformed spectra ($\log(1/R)$). MC prediction models (Fig. 3a) developed using spectral pre-treatments for non-US (control, WI and B) treated samples (Table 1) had $RMSEP \leq 0.21$ (kg water/kg dry matter), RPD_P values ranging from 4.1 to 6.6 and R^2_P values between 0.94 and 0.98. The best regression model was developed using 27 bands selected using the EMCVS on SD pre-treated $\log(1/R)$ spectra (LV 8, $RMSEP$ 0.14 (kg water/kg dry matter), RPD_P 6.6, R^2_P 0.98). The selected bands (in the spectral ranges of 985-999, 1041-1055, 1132 – 1181, 1216 – 1279, 1370 - 1398, 1405 - 1461, 1510 - 1566, 1615 – 1643 nm) may relate to the 1st and 2nd overtone of O-H stretching, 1st and 2nd overtone of C-H aromatic stretching, to the 2nd overtone of -CH₂ and -CH₃ groups of the protein water interaction, the 1st and 2nd overtone of C-H stretching and bending combination..

MC prediction models (Fig. 3b) developed using spectral pre-treatments for US (US-WI and US-B) treated samples (Table 2) had $RMSEP \leq 0.28$ (kg water/kg dry matter), RPD_P values ranging from 3.3 to 4.8 and R^2_P values between 0.91 and 0.96. The best MC prediction model for US treated samples was developed using 20 bands selected using the EMCVS-SR on the

LD pre-treated log (1/R) spectra (LV 6, RMSEP 0.21 (kg water/kg dry matter), RPD_P 4.3, R²_P 0.95). The selected bands (in the spectral ranges of 1083, 1146 - 1195, 1202 – 1230, 1398, 1405 - 1440, 1559 – 1594 nm) and may be attributed to the 2nd overtone of -CH₂ and -CH₃ groups of protein water interaction, to the 1st overtone of C–H stretching and bending combination, the 1st overtone of -OH stretching and the 1st overtone of aromatic -CH respectively. In general, all the developed models in Tables 1 and 2 performed well and demonstrated the potential of NIR-HSI as a process analytical technology tool for process control applications in the meat industry.

Table 1. Performance of the best PLS-R, EMCVS-SR, VIP, EMCVS-SR, EMCVS-VIP moisture regression models developed for non-US (control, WI, and B) treated samples. The best performing model is highlighted in bold.

Regression Model	Pre-treatment		# Selected bands	# Variables	Calibration			Cross validation			Prediction		
	1st	2nd			RMSEc	RPDc	R ² c	RMSEcv	RPDcv	R ² cv	RMSEP	RPDp	R ² p
Reflectance (R)													
PLS	-	-	102	9	0.19	4.7	95	0.21	4.4	95	0.21	4.3	95
PLS	MS	FD	96	7	0.16	5.6	97	0.19	4.9	96	0.20	4.6	95
EMCVS	V	SD	10	5	0.18	5.0	96	0.19	4.8	96	0.21	4.4	95
VIP	MS	FD	16	5	0.20	4.6	95	0.21	4.2	94	0.20	4.6	95
SR	MS	Ls	46	6	0.16	5.5	97	0.18	5.0	96	0.19	4.7	96
EMCVS-VIP	MS	Ls	65	8	0.15	6.1	97	0.17	5.3	96	0.17	5.2	96
EMCVS-SR	MS	FD	71	7	0.16	5.7	97	0.19	4.9	96	0.19	4.7	96

Log (1/R)

PLS	-	-	102	8	0.18	5.0	96	0.20	4.5	95	0.22	4.1	94
PLS	SD	LD	96	8	0.13	6.7	98	0.16	5.6	97	0.16	5.6	97

EMCVS	SD	-	27	8	0.12	7.3	98	0.14	6.6	98	0.14	6.5	98
		SN					0.			0.			0.
VIP	FD	V	28	6	0.19	4.6	95	0.21	4.3	95	0.19	4.7	96
		As					0.			0.			0.
SR	MS	Ls	20	6	0.17	5.3	97	0.18	4.9	96	0.18	5.0	96
EMCVS-							0.			0.			0.
VIP	SD	-	93	8	0.13	6.8	98	0.15	5.9	97	0.16	5.9	97
EMCVS-	As						0.			0.			0.
SR	Ls	SD	71	8	0.14	6.6	98	0.16	5.7	97	0.17	5.5	97

The calibration data set comprised samples from replicates 1 & 2 (n = 162 (18 (before drying) + 144 (during drying))).

The validation data set comprised samples from replicate 3 (n = 81 (9 (before drying) + 72 (during drying))).

PLS, partial least square; EMCVS, ensemble Monte Carlo variable selection; VIP, variable importance projection; SR, selectivity ratio; MS, median scaled; FD, first derivative; SD, second derivative; SNV, standard normal variate; AsLs, asymmetric least squares; LD, linear detrend; #Bands, wavelengths used for model development; #LVs, latent variables. The best model for non-US treated samples is highlighted in bold.

Table 2. Performance of the best PLS-R, EMCVS, SR, VIP, EMCVS-SR, EMCVS-VIP moisture regression models developed for the US (US-WI, US-B) treated samples. The best performing model is highlighted in bold.

Regression Model	Pre-treatment		# Selected bands	# LV	Calibration			Cross validation			Prediction		
	1st	2nd			RM SEc	RP Dc	R ² c	RM SEcv	RP Dcv	R ² cv	RM SEp	RP Dp	R ² p
Reflectance (R)													
PLS	-	-	102	5	0.25	3.7	3	0.28	3.3	91	0.28	3.3	1
							0.			0.			0.
PLS	S	As					9			0.			9
	D	Ls	96	5	0.20	4.6	5	0.22	4.2	94	0.21	4.6	5
							0.			0.			0.
EMCVS	As	SN					9			0.			9
	Ls	V	10	6	0.21	4.6	5	0.23	4.2	94	0.19	4.8	6
							0.			0.			0.
VIP	F	SN					9			0.			9
	D	V	5	4	0.22	4.4	5	0.23	4.1	94	0.21	4.3	5
							0.			0.			0.
SR	T	As					9			0.			9
	D	Ls	21	3	0.21	4.4	5	0.23	4.2	94	0.22	4.3	5
	S						0.			0.			0.
EMCVS-	N						9			0.			9
VIP	V	-	80	7	0.20	4.7	5	0.23	4.1	94	0.21	4.5	5
EMCVS-	M						0.			0.			0.
SR	S	LD	22	6	0.23	4.2	9	0.25	3.9	93	0.21	4.3	9

													4	5
Log (1/R)														
								0.					0.	
								9					9	
PLS	-	-	102	6	0.21	4.6	5	0.24	3.9	93	0.24	4.0	4	
								0.					0.	
	L							9					9	
PLS	D	FD	96	6	0.18	5.3	6	0.20	4.8	96	0.21	4.5	5	
								0.					0.	
	As							9					9	
EMCVS	Ls	-	22	5	0.18	5.2	6	0.20	4.8	96	0.23	4.0	4	
								0.					0.	
	M							9					9	
VIP	S	TD	16	5	0.19	4.9	6	0.21	4.4	95	0.23	4.1	4	
								0.					0.	
	M							9					9	
SR	S	TD	46	4	0.18	5.2	6	0.20	4.7	95	0.23	4.0	4	
								0.					0.	
	As							9					9	
EMCVS- VIP	Ls	-	52	7	0.17	5.5	7	0.20	4.7	95	0.21	4.3	5	
								0.					0.	
	L							9					9	
EMCVS- SR	D	-	20	6	0.18	5.2	6	0.20	4.7	95	0.21	4.3	5	

The calibration data set comprised samples from replicates 1 & 2 (n = 104 (8 (before drying) + 96 (during drying))).

The validation data set comprised samples from replicate 3 (n = 53 (5 (before drying) + 48 (during drying))).

PLS, partial least square; EMCVS, ensemble Monte Carlo variable selection; VIP, variable importance projection; SR, selectivity ratio; MS, median scaled; FD, first derivative; SD, second derivative; TD, third derivative, SNV, standard normal variate; AsLs, asymmetric least squares; LD, linear detrend; #Bands, wavelengths used for model development; #LVs, latent variables. The best model for US treated samples is highlighted in bold.

3.3.1. Moisture content prediction maps

The best performing regression models for non-US (control, WI and B) and US (US-WI and US-B) treated samples were used to develop moisture content (kg water/kg dry matter) prediction maps shown in Fig. 4. Prediction maps were obtained by multiplying the regression coefficient vector of the selected MC prediction model by each pre-treated pixel spectrum in the region of interest (ROI) of each hypercube. It can observe that US-WI samples lost water faster than WI samples during the first 30 min of drying. It can also be observed that the drying profiles of both, B and US-B samples were similar.

4. Conclusions

The potential of NIR-HSI as a process analytical technology tool for the prediction of moisture content during the drying process of beef jerky with and without US treatment and whether brined or not was demonstrated in this study. Ultrasound treatment accelerated the drying of water immersed beef jerky but was not shown to enhance the drying of brined samples due to salt-protein-water interaction.

The majority of the moisture content prediction models developed in this work had RPD values > 4 , indicating their suitability for process control applications. The application of spectral pre-treatments and band selection methods improved the performance of moisture content prediction models developed. The band selection methods selected key spectral bands from smoothed $\log(1/R)$ spectra. The best moisture content prediction models were developed using EMCVS band selection method on SD pre-treated $\log(1/R)$ spectra and EMCVS-SR on LD pre-treated $\log(1/R)$ spectra, respectively. Additional studies are recommended to validate the findings of this research prior to industry adoption.

Acknowledgements

The authors acknowledge funding for this project from FIRM (13/FM/508) as administered by the Irish Department of Agriculture, Food & the Marine.

Competing Interests Statement

The authors, Eva Maria Achata, Carlos Esquerre, K. Shikha Ojha, Brijesh Tiwari & Colm P. O'Donnell declare that they have no known competing financial interests or personal relationships that could have appeared to influence the work reported in this paper.

CRedit authorship contribution statement

E.M. Achata: Investigation, Methodology, Data curation, Formal analysis, Visualization, Writing - original draft.

C.A. Esquerre: Software, Writing - review & editing.

K.S. Ojha: Methodology.

B.K. Tiwari: Conceptualization, Methodology, Resources.

C.P. O'Donnell: Conceptualization, Resources, Writing - review & editing, Supervision, Funding acquisition.

Appendix 1. Moisture content (kg water/kg dry matter) of beef jerky samples.

Time (min)	Control		WI		B		US-WI		US-B	
	Avera ge	S.De v.	Avera ge	S.De v.	Avera ge	S.De v.	Avera ge	S.De v.	Avera ge	S.De v.
0	2.76	0.07	2.97	0.15	2.92	0.17	3.10	0.08	2.88	0.14
30	1.35	0.13	1.75	0.29	1.64	0.33	1.19	0.36	1.77	0.31
60	0.68	0.14	1.14	0.39	0.93	0.12	0.73	0.31	0.97	0.24
90	0.25	0.02	0.58	0.17	0.53	0.14	0.24	0.04	0.57	0.10
120	0.14	0.08	0.31	0.09	0.34	0.03	0.20	0.06	0.41	0.08
150	0.10	0.05	0.19	0.09	0.26	0.01	0.12	0.07	0.32	0.05
180	0.08	0.04	0.15	0.10	0.19	0.06	0.10	0.06	0.24	0.02
210	0.10	0.07	0.11	0.02	0.16	0.07	0.10	0.06	0.12	0.05
240	0.11	0.03	0.09	0.03	0.09	0.07	0.11	0.04	0.08	0.04

B; brined samples

WI; water immersed samples

US-B; brined samples with ultrasound treatment

US-WI; water immersed samples with ultrasound treatment

Appendix 2. Thin layer drying models investigated.

Model	Parameter	Control	WI	B	US-WI	US-B
Newton (Luckose, et al., 2017)	RMSE	0.019	0.015	0.02	0.031	0.021

MR = exp(-kt)	χ^2	4.09×10^{-4}	2.53×10^{-4}	4.29×10^{-4}	1.10×10^{-3}	4.92×10^{-3}
	AICc	-	-	-	-	-
	Dif AICc	44.166	48.486	43.729	35.294	42.502
	R ²	1	1	1274.681	20.539	1
	R ²	0.996	0.998	0.996	0.989	0.995
	K	3.99×10^{-4}	2.89×10^{-4}	3.06×10^{-4}	4.59×10^{-4}	2.79×10^{-4}
<hr/>						
Page (Luckose, et al., 2017)	RMSE	0.019	0.015	0.013	0.019	0.019
MR = exp(-ktn)	χ^2	4.66×10^{-4}	2.79×10^{-4}	2.23×10^{-4}	4.89×10^{-4}	4.61×10^{-4}
	AICc	-	-	-48.39	-	-
	Dif AICc	41.756	46.372	123.935	41.338	41.852
	R ²	3.336	2.875	5	1	1.384
	R ²	0.996	0.998	0.998	0.996	0.996
	K	9.91×10^{-1}	1.02×10^0	8.87×10^{-1}	7.52×10^{-1}	9.34×10^{-1}
	n	0.934	1.022	0.887	0.752	0.934
	<hr/>					
Henderson and Pabis (Luckose, et al., 2017)	RMSE	0.019	0.015	0.019	0.031	0.021
MR = a exp(-kt)	χ^2	4.67×10^{-4}	2.89×10^{-4}	4.75×10^{-4}	1.23×10^{-3}	5.60×10^{-4}
	AICc	-	-	-	-	-40.11
	Dif AICc	41.737	46.073	41.587	33.054	3718.876
	R ²	3.368	3.342	76	62.953	3.306
	R ²	0.996	0.998	0.996	0.989	0.995
	K	3.99×10^{-4}	2.89×10^{-4}	3.03×10^{-4}	4.53×10^{-4}	2.78×10^{-4}
	a	1	1.002	0.99	0.987	0.996
	<hr/>					
Logarithmic (Luckose, et al., 2017)	RMSE	0.014	0.015	0.006	0.021	0.016
MR = a exp(-kt) + c	χ^2	3.03×10^{-4}	3.32×10^{-4}	5.85×10^{-5}	6.43×10^{-4}	3.64×10^{-4}
	AICc	-	-	-	-	-
	Dif AICc	43.219	42.405	58.029	36.448	41.576
	R ²	1.605	20.909	1	11.535	1.589
	R ²	0.998	0.998	1	0.995	0.997
	K	4.26×10^{-4}	2.92×10^{-4}	3.41×10^{-4}	5.12×10^{-4}	3.06×10^{-4}
	a	0.984	0.999	0.965	0.96	0.976
	c	0.02	0.004	0.035	0.034	0.03
<hr/>						
Two term (Luckose, et al., 2017)	RMSE	0.01	0.015	0.006	0.02	0.015

MR = a exp(-kot) + b exp(-k1t)	χ^2	1.95×10^{-4}	4.04×10^{-4}	6.33×10^{-5}	7.27×10^{-4}	4.22×10^{-4}	
	AICc	-	-	-	-	-	
	Dif AICc	2.146	817.662	13.974	195.936	30.199	
	R ²	0.999	0.998	1	0.996	0.998	
	K	4.06×10^{-4}	2.89×10^{-4}	3.53×10^{-4}	1.19×10^{-4}	7.20×10^{-5}	
	K2	2.88×10^{-4}	2.89×10^{-4}	4.48×10^{-5}	5.83×10^{-4}	3.23×10^{-4}	
	a	1.002	0.501	0.937	0.126	0.084	
	b	0.001	0.501	0.065	0.871	0.923	
	<hr/>						
Wang and Singh (Toğrul & Pehlivan, 2003)	RMSE	0.077	0.076	0.064	0.097	0.06	
MR = 1+ at + bt	χ^2	7.61×10^{-3}	2.70×10^{-3}	5.26×10^{-3}	1.21×10^{-2}	4.69×10^{-3}	
	AICc	-1.82	-	-	-5.625	-	
	Dif AICc	2.86×10^7	2.35×10^6	5.59×10^9	5.69×10^7	1.41×10^6	
	R ²	0.938	0.979	0.956	0.896	0.961	
	a	0.88	0.93	0.903	0.836	0.918	
	b	1.84×10^{-4}	1.71×10^{-4}	1.67×10^{-4}	1.77×10^{-4}	1.63×10^{-4}	
	<hr/>						
	Simplified Fick's diffusion equation (Luckose, et al., 2017)	RMSE	0.019	0.015	0.019	0.031	0.021
MR = a exp(-c(t/L2))	χ^2	4.67×10^{-4}	2.89×10^{-4}	4.75×10^{-4}	1.23×10^{-3}	5.60×10^{-4}	
	AICc	-	-	-	-	-39.11	
	Dif AICc	5.552	5.509	6131.39	103.792	5.451	
	R ²	0.996	0.998	0.996	0.989	0.995	
	K	8.98×10^{-10}	6.51×10^{-10}	6.82×10^{-10}	1.02×10^{-10}	6.27×10^{-10}	
	a	1	1.002	0.99	0.987	0.996	
	<hr/>						
Modified Page (Luckose, et al., 2017)	RMSE	0.187	0.248	0.231	0.156	0.252	
MR = exp(-k(t/L2)n)	χ^2	0.045	0.079	0.069	0.031	0.082	
	AICc	1.378	6.439	5.156	-1.923	6.732	
	Dif AICc	7.76×10^9	8.45×10^{11}	5.25×10^{13}	3.62×10^8	4.91×10^{10}	
	R ²	0.634	0.374	0.422	0.732	0.325	
	K	6.00×10^{-5}	6.00×10^{-5}	6.00×10^{-5}	6.00×10^{-5}	6.00×10^{-5}	
	<hr/>						

	n	1	1	1	1	1
Modified Henderson and Pabis (Toğrul, et al., 2003)	RMSE	0.01	0.015	0.006	0.019	0.015
MR = a exp(-kt) + b exp(-gt) + c exp(-ht)	χ^2	3.25×10^{-4}	6.74×10^{-4}	1.06×10^{-4}	1.04×10^{-3}	7.03×10^{-4}
	AICc	-7.638	0.927	17.755	2.807	-0.686
	Dif AICc	8.55×10^7	5.37×10^{10}	5.57×10^8	3.85×10^9	1.20×10^9
	R ²	0.999	0.998	1	0.996	0.998
	K	4.06×10^{-4}	2.89×10^{-4}	4.48×10^{-5}	1.46×10^{-6}	3.23×10^{-4}
	a	0.501	0.334	0.065	0.173	0.462
	b	0.501	0.334	0.463	0.639	0.46
	c	0	0	0	0.001	0
	g	0.001	0.334	0.474	0.187	0.084
	h	2.58×10^{-7}	2.89×10^{-4}	3.53×10^{-4}	1.79×10^{-4}	7.21×10^{-5}
Verma (Toğrul, et al., 2003)	RMSE	0.186	0.132	0.14	0.2	0.124
MR= a exp(-kt) + (1- a)exp(-gt)	χ^2	5.21×10^{-2}	2.60×10^{-2}	2.93×10^{-2}	5.98×10^{-2}	2.32×10^{-2}
	AICc	4.104	-2.147	-1.075	5.346	-3.197
	Dif AICc	3.03×10^{10}	1.15×10^{10}	2.33×10^{12}	1.37×10^{10}	3.43×10^8
	R ²	0.637	0.823	0.788	0.56	0.836
	K	6.00×10^{-5}	6.00×10^{-5}	6.00×10^{-5}	6.00×10^{-5}	6.00×10^{-5}
	a	1.43×10^5	1.37×10^5	1.51×10^5	1.61×10^5	1.47×10^5
	g	6.00×10^{-5}	6.00×10^{-5}	6.00×10^{-5}	6.00×10^{-5}	6.00×10^{-5}

WI, water immersed samples; B, brined samples; US-WI, water immersed samples with ultrasound treatment; US-B, brined samples with ultrasound treatment;; RMSE, root mean square error of prediction; χ^2 , reduced chi-square; AICc, Akaike information criterion; R², correlation coefficient squared; K,a,b,c,g,h,n, constants; MR, moisture ratio; t, time; L2, sample thickness.

References

- Achata, E. M., Esquerre, C. A., Gowen, A. A., & O'Donnell, C. P. (2018). Feasibility of near infrared and Raman hyperspectral imaging combined with multivariate analysis to assess binary mixtures of food powders. *Powder Technology*, 336, 555-566.
- Achata, E. M., Esquerre, C. A., O'Donnell, C. P., & Gowen, A. A. (2015). A study on the application of near infrared hyperspectral chemical imaging for monitoring moisture content and water activity in low moisture systems. *Molecules*, 20(2), 2611.

- Achata, E. M., Inguglia, E. S., Esquerre, C. A., Tiwari, B. K., & O'Donnell, C. P. (2019). Evaluation of Vis-NIR hyperspectral imaging as a process analytical tool to classify brined pork samples and predict brining salt concentration. *Journal of Food Engineering*, *246*, 134-140.
- Altas, M. C., Kudryashov, E., & Buckin, V. (2016). Ultrasonic Monitoring of Enzyme Catalysis; Enzyme Activity in Formulations for Lactose-Intolerant Infants. *Analytical Chemistry*, *88*(9), 4714-4723.
- Andersen, M.-B. S., Frydenvang, J., Henckel, P., & Rinnan, Å. (2016). The potential of laser-induced breakdown spectroscopy for industrial at-line monitoring of calcium content in comminuted poultry meat. *Food Control*, *64*, 226-233.
- Andueza, D., Agabriel, C., Constant, I., Lucas, A., & Martin, B. (2013). Using visible or near infrared spectroscopy (NIRS) on cheese to authenticate cow feeding regimes. *Food Chemistry*, *141*(1), 209-214.
- Başlar, M., Kılıçlı, M., Toker, O. S., Sağdıç, O., & Arici, M. (2014). Ultrasonic vacuum drying technique as a novel process for shortening the drying period for beef and chicken meats. *Innovative Food Science & Emerging Technologies*, *26*, 182-190.
- Burger, J., & Gowen, A. (2011). Data handling in hyperspectral image analysis. *Chemometrics and Intelligent Laboratory Systems*, *108*(1), 13-22.
- Cadet, F., Pin, F. W., Rouch, C., Robert, C., & Baret, P. (1995). Enzyme kinetics by mid-infrared spectroscopy: β -fructosidase study by a one-step assay. *Biochimica et Biophysica Acta (BBA) - Protein Structure and Molecular Enzymology*, *1246*(2), 142-150.
- Chong, I.-G., & Jun, C.-H. (2005). Performance of some variable selection methods when multicollinearity is present. *Chemometrics and Intelligent Laboratory Systems*, *78*(1), 103-112.
- Corrêa, J. L. G., Rasia, M. C., Mulet, A., & Cárcel, J. A. (2017). Influence of ultrasound application on both the osmotic pretreatment and subsequent convective drying of pineapple (*Ananas comosus*). *Innovative Food Science & Emerging Technologies*, *41*, 284-291.
- Cullen, P. J., O'Donnell, C. P., & Fagan, C. C. (2014). Benefits and Challenges of Adopting PAT for the Food Industry. In C. P. O'Donnell, C. C. Fagan & P. J. Cullen (Eds.), *Process Analytical Technology for the Food Industry* (pp. 1-5). New York: Springer-Verlag.
- Esquerre, C., Gowen, A. A., Burger, J., Downey, G., & O'Donnell, C. P. (2012). Suppressing sample morphology effects in near infrared spectral imaging using chemometric data pre-treatments. *Chemometrics and Intelligent Laboratory Systems*, *117*, 129-137.
- Esquerre, C., Gowen, A. A., Downey, G., & O'Donnell, C. P. (2011). Selection of variables based on most stable normalized partial least squares regression coefficients in an ensemble Monte Carlo procedure. *Journal of Near Infrared Spectroscopy*, *19*(6), 443-450.
- Esquerre, C. A., Gowen, A. A., O'Gorman, A., Downey, G., & O'Donnell, C. P. (2017). Evaluation of ensemble Monte Carlo variable selection for identification of metabolite markers on NMR data. *Analytica Chimica Acta*, *964*, 45-54.
- Fernandes, F. A. N., Rodrigues, S., García-Pérez, J. V., & Cárcel, J. A. (2016). Effects of ultrasound-assisted air-drying on vitamins and carotenoids of cherry tomatoes. *Drying Technology*, *34*(8), 986-996.
- Food and Drug Administration. (2004). Guidance for Industry PAT — A Framework for Innovative Pharmaceutical Development, Manufacturing, and Quality Assurance. In F. a. D. Administration (Ed.).
- García-Pérez, J. V., Cárcel, J. A., Benedito, J., & Mulet, A. (2007). Power Ultrasound Mass Transfer Enhancement in Food Drying. *Food and Bioproducts Processing*, *85*(3), 247-254.
- Gowen, A., Burger, J., Esquerre, C., Downey, G., & O'Donnell, C. (2014). Near infrared hyperspectral image regression: On the use of prediction maps as a tool for detecting model overfitting. *Journal of Near Infrared Spectroscopy*, *22*(4), 261-270.

- Gowen, A. A., Downey, G., Esquerre, C., & O'Donnell, C. P. (2011). Preventing over-fitting in PLS calibration models of near-infrared (NIR) spectroscopy data using regression coefficients. *Journal of Chemometrics*, *25*(7), 375-381.
- Hammami, M., Rouissi, H., Salah, N., Selmi, H., Al-Otaibi, M., Blecker, C., & Karoui, R. (2010). Fluorescence spectroscopy coupled with factorial discriminant analysis technique to identify sheep milk from different feeding systems. *Food Chemistry*, *122*(4), 1344-1350.
- Huang, H., Yu, H., Xu, H., & Ying, Y. (2008). Near infrared spectroscopy for on/in-line monitoring of quality in foods and beverages: A review. *Journal of Food Engineering*, *87*(3), 303-313.
- Jones, L. J., Upson, R. H., Haugland, R. P., Panchuk-Voloshina, N., Zhou, M., & Haugland, R. P. (1997). Quenched BODIPY Dye-Labeled Casein Substrates for the Assay of Protease Activity by Direct Fluorescence Measurement. *Analytical Biochemistry*, *251*(2), 144-152.
- Karmali, K., Karmali, A., Teixeira, A., & Curto, M. J. M. (2004). Assay for glucose oxidase from *Aspergillus niger* and *Penicillium amagasakiense* by Fourier transform infrared spectroscopy. *Analytical Biochemistry*, *333*(2), 320-327.
- Karunathilaka, S. R., Yakes, B. J., He, K., Chung, J. K., & Mossoba, M. (2018). Non-targeted NIR spectroscopy and SIMCA classification for commercial milk powder authentication: A study using eleven potential adulterants. *Heliyon*, *4*(9), e00806.
- Kowalski, S. J., & Rybicki, A. (2017). Ultrasound in wet biological materials subjected to drying. *Journal of Food Engineering*, *212*, 271-282.
- Kroehnke, J., Szadzińska, J., Stasiak, M., Radziejewska-Kubzdela, E., Biegańska-Marecik, R., & Musielak, G. (2018). Ultrasound- and microwave-assisted convective drying of carrots – Process kinetics and product's quality analysis. *Ultrasonics Sonochemistry*, *48*, 249-258.
- Kuehler, C. A., & Stine, C. M. (1974). EFFECT OF ENZYMIC HYDROLYSIS ON SOME FUNCTIONAL PROPERTIES OF WHEY PROTEIN. *Journal of Food Science*, *39*(2), 379-382.
- Kumar, S., & Barth, A. (2010). Following Enzyme Activity with Infrared Spectroscopy. *Sensors*, *10*(4).
- Lieske, B. r., & Konrad, G. (1996). Physico-chemical and functional properties of whey protein as affected by limited papain proteolysis and selective ultrafiltration. *International Dairy Journal*, *6*(1), 13-31.
- Lin, J., & Brown, C. W. (1992). Near-IR Spectroscopic Determination of NaCl in Aqueous Solution. *Applied Spectroscopy*, *46*(12), 1805-1815.
- Luckose, F., Pandey, M. C., & Harnali, P. T. (2017). Effect of sodium chloride reduction on drying kinetics of restructured chicken jerky. *Food Bioscience*, *19*, 156-162.
- Magalhães, M. L., Cartaxo, S. J. R., Gallão, M. I., García-Pérez, J. V., Cárcel, J. A., Rodrigues, S., & Fernandes, F. A. N. (2017). Drying intensification combining ultrasound pre-treatment and ultrasound-assisted air drying. *Journal of Food Engineering*, *215*, 72-77.
- Munera, S., Amigo, J. M., Plasco, J., Cubero, S., Talens, P., & Aleixos, N. (2017). Ripeness monitoring of two cultivars of nectarine using VIS-NIR hyperspectral reflectance imaging. *Journal of Food Engineering*, *214*, 29-39.
- Nian, Y., Zhao, M., O'Donnell, C. P., Downey, G., Kerry, J. P., & Allen, P. (2017). Assessment of physico-chemical traits related to eating quality of young dairy bull beef at different ageing times using Raman spectroscopy and chemometrics. *Food Research International*, *99*, 778-789.
- Ojha, K. S., Granato, D., Rajuria, G., Barba, F. J., Kerry, J. P., & Tiwari, B. K. (2018). Application of chemometrics to assess the influence of ultrasound frequency, *Lactobacillus sakei* culture and drying on beef jerky manufacture: Impact on amino acid profile, organic acids, texture and colour. *Food Chemistry*, *239*, 544-550.
- Ojha, S. K., Kerry, J. P., & Tiwari, B. K. (2017). Investigating the influence of ultrasound pre-treatment on drying kinetics and moisture migration measurement in *Lactobacillus sakei* cultured and uncultured beef jerky. *LWT - Food Science and Technology*, *81*, 42-49.
- Osborne, B. G., Fearn, T., & Hindle, P. T. (1993). *Practical NIR spectroscopy with applications in food and beverage analysis*. Essex, England: Longman Scientific & Technical ; Wiley.

- Rajalahti, T., Arneberg, R., Kroksveen, A. C., Berle, M., Myhr, K.-M., & Kvalheim, O. M. (2009). Discriminating Variable Test and Selectivity Ratio Plot: Quantitative Tools for Interpretation and Variable (Biomarker) Selection in Complex Spectral or Chromatographic Profiles. *Analytical Chemistry*, *81*(7), 2581-2590.
- Resa, P., & Buckin, V. (2011). Ultrasonic analysis of kinetic mechanism of hydrolysis of cellobiose by β -glucosidase. *Analytical Biochemistry*, *415*(1), 1-11.
- Rojas, M. L., & Augusto, P. E. D. (2018). Ethanol and ultrasound pre-treatments to improve infrared drying of potato slices. *Innovative Food Science & Emerging Technologies*, *49*, 65-75.
- Schindler, R., Le Thanh, H., Lendl, B., & Kellner, R. (1998). Determination of enzyme kinetics and chemometric evaluation of reaction products by FTIR spectroscopy on the example of β -fructofuranosidase. *Vibrational Spectroscopy*, *16*(2), 127-135.
- Senesi, G. S., Dell'Aglio, M., Gaudiuso, R., De Giacomo, A., Zaccone, C., De Pascale, O., Miano, T. M., & Capitelli, M. (2009). Heavy metal concentrations in soils as determined by laser-induced breakdown spectroscopy (LIBS), with special emphasis on chromium. *Environmental Research*, *109*(4), 413-420.
- Siró, I., Vén, C., Balla, C., Jónás, G., Zeke, I., & Friedrich, L. (2009). Application of an ultrasonic assisted curing technique for improving the diffusion of sodium chloride in porcine meat. *Journal of Food Engineering*, *91*(2), 353-362.
- Slattery, H., & Fitzgerald, R. J. (1998). Functional Properties and Bitterness of Sodium Caseinate Hydrolysates Prepared with a Bacillus Proteinase. *Journal of Food Science*, *63*(3), 418-422.
- Spellman, D., McEvoy, E., O'Cuinn, G., & FitzGerald, R. J. (2003). Proteinase and exopeptidase hydrolysis of whey protein: Comparison of the LIBS, OPA and pH stat methods for quantification of degree of hydrolysis. *International Dairy Journal*, *13*(6), 447-453.
- Tao, Y., Zhang, J., Jiang, S., Xu, Y., Show, P.-L., Han, Y., Ye, X., & Ye, M. (2018). Contacting ultrasound enhanced hot-air convective drying of garlic slices: Mass transfer modeling and quality evaluation. *Journal of Food Engineering*, *235*, 79-88.
- Toğrul, İ. T., & Pehlivan, D. (2003). Modelling of drying kinetics of single apricot. *Journal of Food Engineering*, *58*(1), 23-32.
- Vega-Gálvez, A., Puente-Díaz, L., Lemus-Mondaca, R., Miranda, M., & Torres, M. J. (2014). Mathematical Modeling of Thin-Layer Drying Kinetics of Cape Gooseberry (*Physalis peruviana* L.). *Journal of Food Processing and Preservation*, *38*(2), 728-736.
- Williams, P. (2014). The RPD Statistic: A Tutorial Note. *NIR news*, *25*(1), 22-26.
- Zhao, M., Downey, G., & O'Donnell, C. P. (2014). Detection of adulteration in fresh and frozen beefburger products by beef offal using mid-infrared ATR spectroscopy and multivariate data analysis. *Meat Science*, *96*(2, Part A), 1003-1011.
- Zhao, M., Downey, G., & O'Donnell, C. P. (2015). Dispersive Raman Spectroscopy and Multivariate Data Analysis To Detect Offal Adulteration of Thawed Beefburgers. *Journal of Agricultural and Food Chemistry*, *63*(5), 1433-1441.

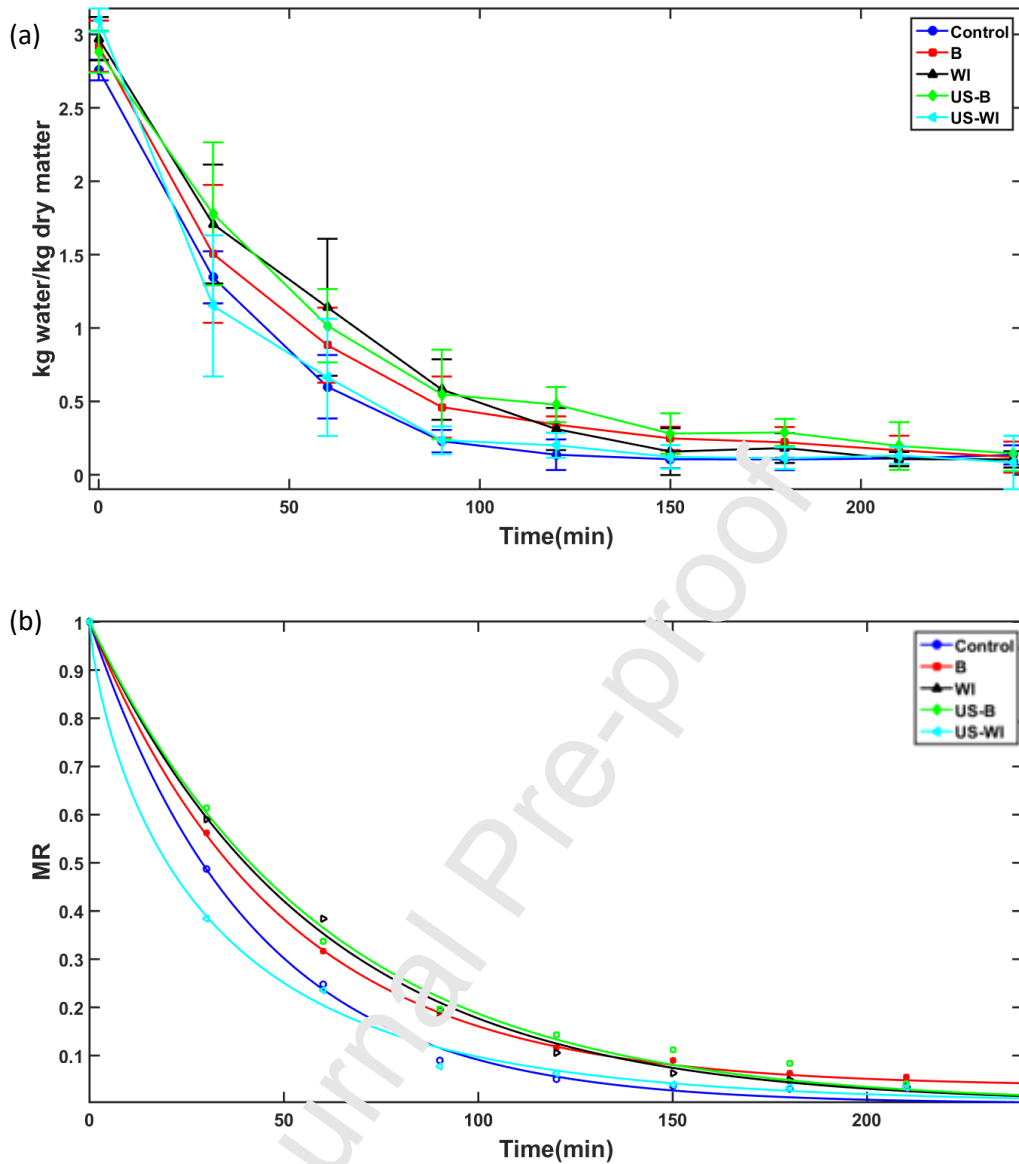


Figure 1: Drying kinetics of beef jerky for all experimental treatments (a) moisture content (kg water/kg dry matter) (b) predicted moisture ratio (MR).

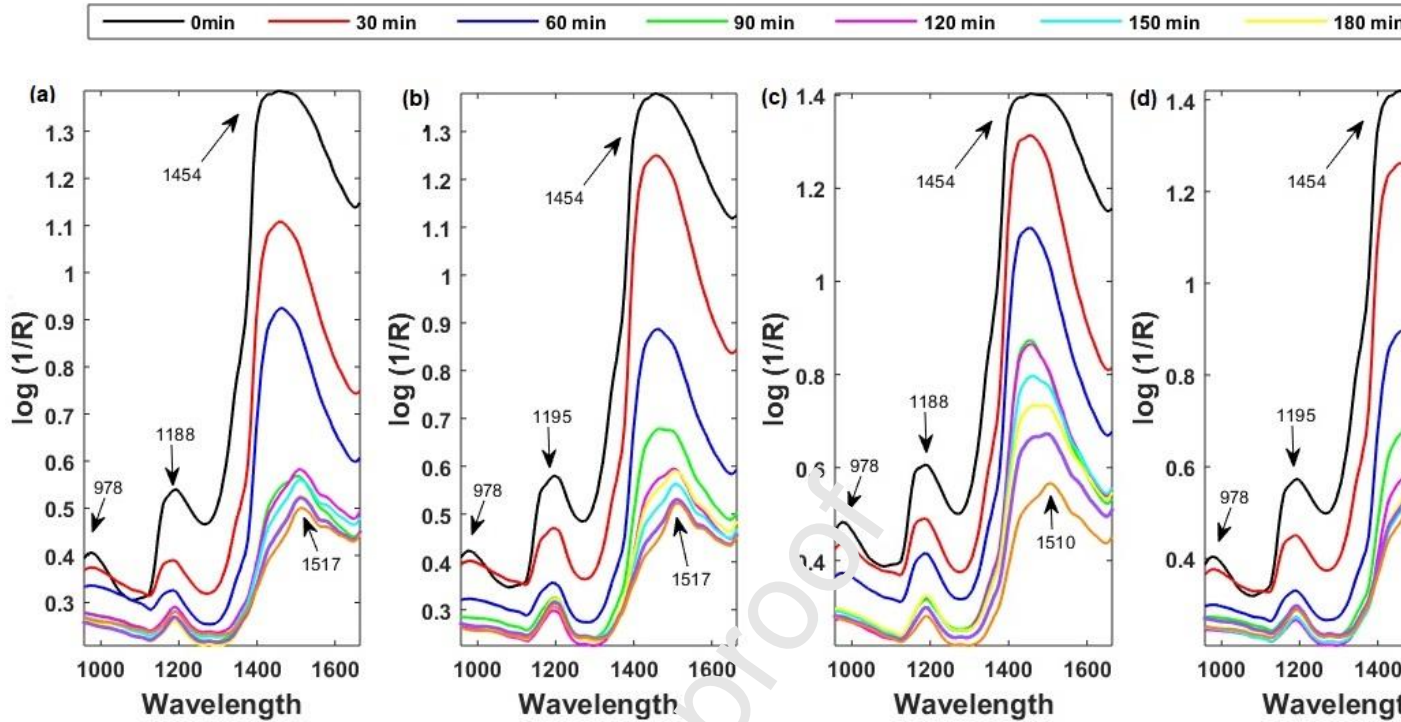


Figure 2: SG smoothed mean $\log(1/R)$ spectra of beef jerky at selected drying times for all samples, (a) Control samples (b) WI, (c) B, (d) US-WI, (e) US-B.

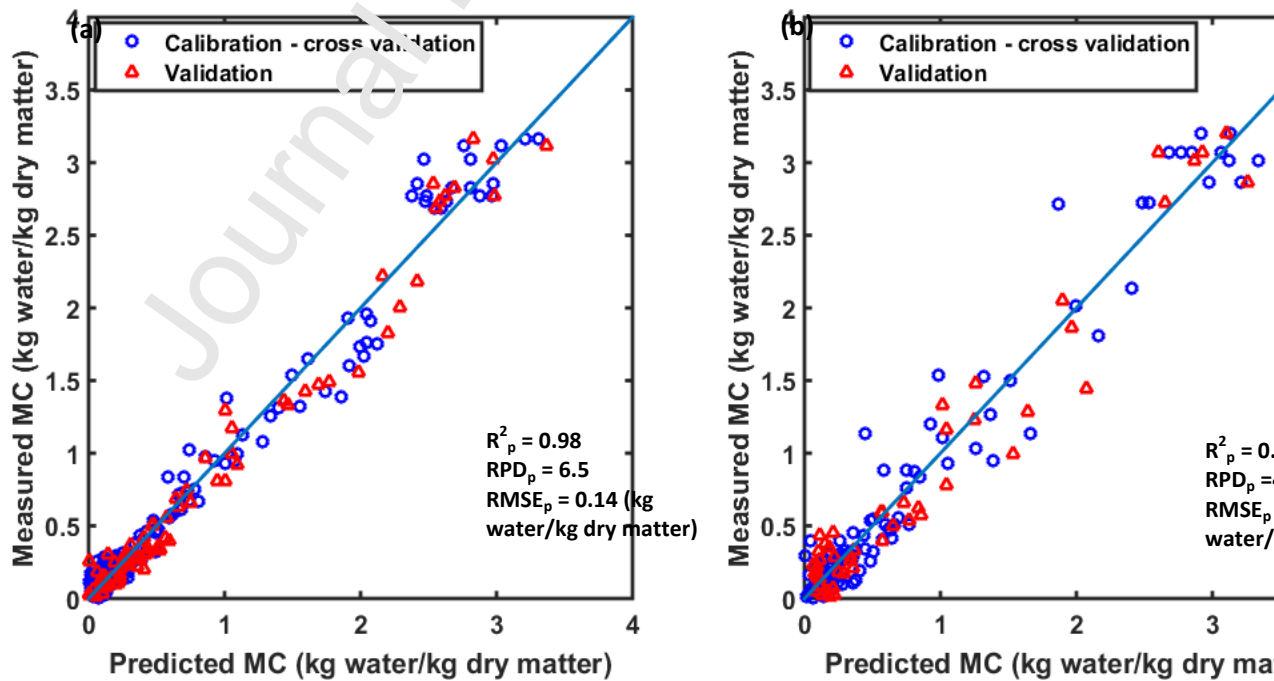


Figure 3: Moisture content (kg water/kg dry matter) prediction models developed using the best regression models a) EMCVS on the SD pre-treated $\log(1/R)$ spectra, for control, WI and B samples and b) EMCVS-SR on the LD pre-treated $\log(1/R)$ spectra for US-WI and US-B

samples. $RMSEP$, root mean square error of prediction; R^2_P , coefficient of determination; RPD_P , residual prediction deviation.

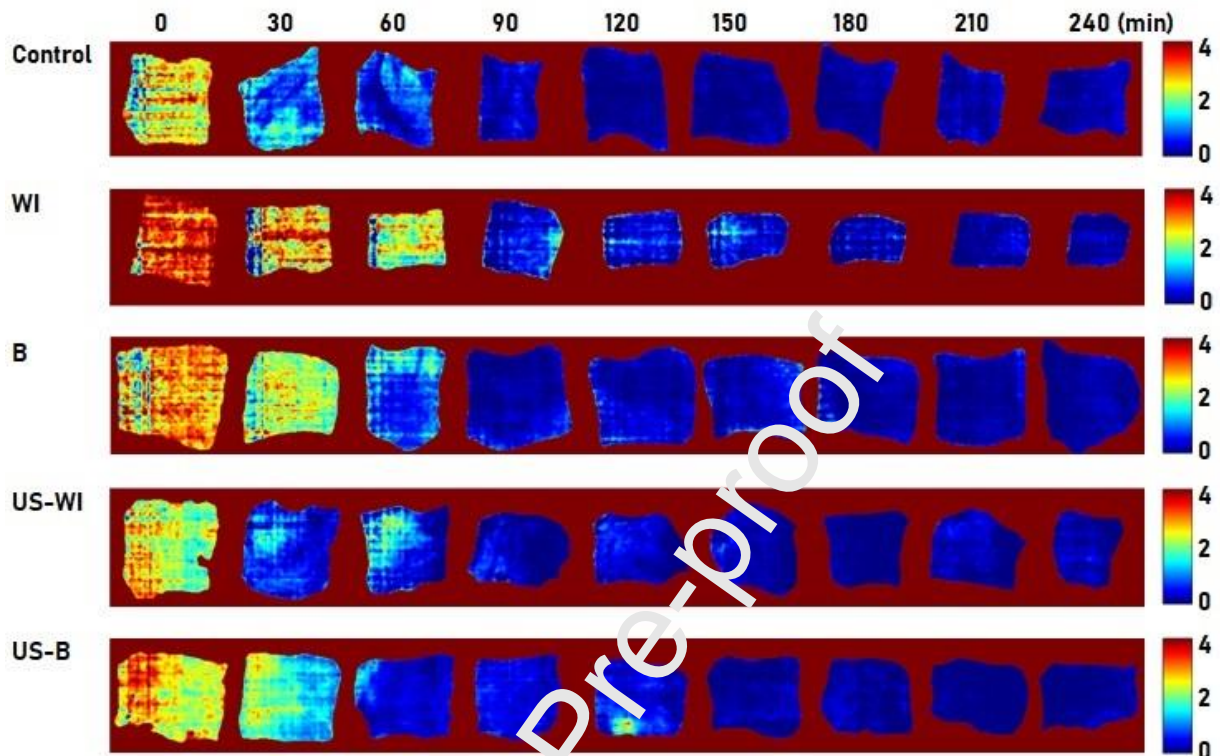


Figure 4: Moisture content (kg water/kg dry matter) prediction maps developed using the best regression models (EMCVS or the SD pre-treated $\log(1/R)$ spectra) for control, WI and B samples and EMCVS-SR on the IL pre-treated $\log(1/R)$ spectra for US-WI and US-B. The colour scale for moisture content (kg water/kg dry matter) varies from 1 (blue) for low moisture samples to 3 (burgundy) for high moisture samples.

Highlights

- Application of NIR hyperspectral imaging to predict beef jerky moisture content.
- Band selection and spectral pre-treatments improved moisture prediction models.
- Effect of ultrasound on drying kinetics of beef jerky demonstrated.
- Hyperspectral imaging is suitable for process control of beef jerky processing.